



ELSEVIER

Journal of Nuclear Materials 290–293 (2001) 89–93

journal of  
nuclear  
materials

www.elsevier.nl/locate/jnucmat

# Mixed-material coating formation on tungsten surfaces during plasma exposure in TEXTOR-94

D. Hildebrandt <sup>a,\*</sup>, P. Wienhold <sup>b</sup>, W. Schneider <sup>a</sup>

<sup>a</sup> EURATOM Association, Max-Planck-Institut für Plasmaphysik, Bereich Plasmadiagnostik, Mohrenstrasse 40/41, D-10117 Berlin, Germany

<sup>b</sup> Institut für Plasmaphysik, Forschungszentrum Jülich GmbH, EURATOM Association, D-52425 Jülich, Germany

## Abstract

A polished graphite sample with a tungsten layer on the plasma-facing surface was exposed to the scrape-off plasma of TEXTOR-94 for about 200 s of discharge time. The plasma exposure caused a contamination layer with a thickness up to 300 nm consisting mainly of the deposited plasma impurity carbon and the tungsten substrate material. The processes and conditions involved in the growth of such mixed material layers are examined. In accompanying experiments, the penetration of carbon into tungsten by diffusion and ion implantation at different temperatures has been measured. The influence of synergistic effects on the carbon penetration into tungsten by the simultaneous impact of carbon and hydrogen ions was studied by irradiation of tungsten with CH<sub>3</sub> ions. The discussion also includes processes such as non-uniform deposition, preferential erosion and prompt local redeposition. © 2001 Elsevier Science B.V. All rights reserved.

*Keywords:* Material mixing; Carbon; Tungsten; Diffusion; Erosion; Redeposition

## 1. Introduction

The plasma impact on any material causes a modification of its original surface by deposition and erosion processes. Arising from the simultaneous use of different materials as plasma-facing components in magnetic fusion devices, mixed material effects are expected. Post-mortem investigation of tungsten divertor tiles of ASDEX-Upgrade showed a surface contamination with a layer thickness up to several  $\mu\text{m}$  [1,2]. This surface layer consists mainly of the deposited plasma impurities carbon and boron and the hydrogenic isotopes but also contains considerable amount of the tungsten substrate material. In regions with intensive plasma-material interaction located near the strike line of outer divertor tiles, atomic surface concentrations of tungsten up to 30% have been measured at carbon deposition of about  $10^{21}$ – $10^{22}$  C-atoms  $\text{m}^{-2}$ . On inner divertor tiles, tungsten is still present at the surface with an atomic concentration of 2% even after deposition of  $10^{23}$ – $10^{24}$  C-atoms  $\text{m}^{-2}$ .

In the present paper, the processes and conditions involved in the growth of mixed material layers on tungsten surfaces are experimentally examined. In a plasma experiment, a graphite sample with a multi-layer coating was exposed to the scrape-off plasma of TEXTOR-94. The plasma-facing surface of the sample was covered with a tungsten layer. A part of the tungsten layer was protected by a carbon layer. This allowed a direct comparison of erosion and deposition effects on tungsten and carbon under equal plasma conditions [3].

After the exposure to the carbon-contaminated scrape-off plasma of TEXTOR-94, the surface composition of the sample was investigated using surface analysis techniques, in particular with respect to the spatial distribution of carbon and tungsten.

In the accompanying experiments, the depth distribution of carbon and tungsten have been measured after annealing a tungsten layer covered with a carbon film and after ion implantation of carbon into tungsten at different substrate temperatures. The influence of synergistic effects on the carbon penetration into tungsten as occurring during plasma exposure by the simultaneous impact of carbon and hydrogen ions has been studied by irradiation of tungsten with CH<sub>3</sub> ions.

\* Corresponding author. Tel.: +49-30 203 66 164; fax: +49-30 203 66 111.

E-mail address: dth@ipp.mpg.de (D. Hildebrandt).

## 2. Experimental details

### 2.1. Plasma experiment in TEXTOR-94

For this experiment, a polished sample of fine-grained graphite (size  $110 \times 75 \text{ mm}^2$ , 2 mm thick) with a tungsten layer of 300 nm thickness was used (see also [4]). The W layer was separated from the graphite substrate by a 200 nm thick rhenium layer to avoid diffusion of carbon from the bulk material into the tungsten layer. The major part of the tungsten layer was protected by an amorphous hydrogenated carbon layer (200 nm thick) deposited prior to the exposure in TEXTOR-94 by a glow discharge. Two spots with a diameter of 5 mm and locally separated by 22 mm were not protected by the a-C:H film allowing the direct plasma impact on the tungsten layer.

This specimen was mounted on a graphite probe head and located near the last closed flux surface (LCFS) at  $r_a = 46 \text{ cm}$ . Its upper plane surface was declined by  $20^\circ$  with respect to the toroidal magnetic field and oriented to the ion drift side. A thin Al shield covered a part of the sample in an area far from the plasma keeping the sample surface virgin. Altogether, the probe head with the sample was exposed for 36 NBI-heated discharges with a total exposure time of about 197 s (total duration of NBI phases is about 64 s). During the first two discharges, the probe head was located at  $r = 46.8 \text{ cm}$ . Hence, the radial position of the two W spots was 47.3 and 48.1 cm, respectively. For the other discharges, the probe head was moved further away from the LCFS to  $r = 48.8 \text{ cm}$  to reduce the heat flux to the sample. Plasma edge densities and temperatures were measured by the Li- and He-diagnostics [5].

The electron temperature,  $T_e$ , at a minor radius of 47.3 cm (closest position of a W spot to the LCFS) was about 35 eV at a plasma density  $n$  of  $1 \times 10^{18} \text{ m}^{-3}$  during the ohmic phase and 55 eV at a plasma density of  $1.5 \times 10^{18} \text{ m}^{-3}$  during the NBI-heated phase. The corresponding deuterium ion fluxes,  $\Gamma_D$ , to the inclined surface were  $1 \times 10^{22}$  and  $2 \times 10^{22} \text{ D m}^{-2} \text{ s}^{-1}$ . The e-folding lengths of  $T_e$ ,  $n$  and  $\Gamma_D$  were determined to be 100, 24 and 21 mm for the ohmic phase and 60, 27 and 22 mm for the NBI-heated phase, respectively. The ion temperature is expected to be about 240 eV during the NBI-heated phase. The edge plasma is contaminated by carbon with a concentration of a few percent.

### 2.2. Annealing

In order to investigate the migration of carbon in tungsten by diffusion at elevated temperatures, the virgin part of the graphite sample with the multi-layer coating described in Section 2.1 was annealed by electron bombardment at temperatures 770, 1070 and 1370 K. The desired temperature was reached within 60 s and held for 600 s. Before and after each heating cycle, the surface composition and the depth distribution of car-

bon and tungsten were measured by surface analysis methods described below.

### 2.3. Ion implantation

The specimens for ion implantation were made from solid tungsten and from pyrolytic graphite covered with a tungsten layer of 100 nm thickness, respectively [6].

The implantations to the graphite specimens with the tungsten layer were performed using  $^{13}\text{C}^+$ -ions at an ion energy of 2.4 keV with a fluence of about  $8 \times 10^{22} \text{ C m}^{-2}$ . The temperature of the specimens during implantation were 290, 770 or 970 K.

The solid tungsten specimens were irradiated with 2.4 keV  $^{12}\text{C}^+$  and 3 keV  $\text{CH}_3^+$  (2.4 keV/ $^{12}\text{C}$  atom). These implantations were performed with ion fluences between  $2.6 \times 10^{22}$  and  $9 \times 10^{22} \text{ ions m}^{-2}$  at target temperatures of 290, 770 and 1070 K, respectively.

### 2.4. Analysis methods

All samples were investigated by Auger electron spectroscopy (AES) and secondary ion mass spectrometry (SIMS). AES is done with a primary electron energy of 5 keV. For AES and SIMS depth profiling, an  $\text{O}_2$  ion beam with an energy of 10 keV was used. AES and SIMS have the same analysis area. The diameter of the beam is 1  $\mu\text{m}$  (AES) and about 3  $\mu\text{m}$  (SIMS), respectively. This allows 2D images of the elemental concentration to be taken with a lateral resolution in the  $\mu\text{m}$ -range.

## 3. Results

### 3.1. Plasma-exposed sample

Fig. 1 shows the depth profiles of carbon and tungsten measured by AES at the location of the two tungsten spots and for the a-C:H layer in the area covered by the Al shield during the plasma exposure. The depth profiles of the covered area show a complete carbon film with a narrow interface between the a-C:H layer and the tungsten layer at a depth of 180 nm (Fig. 1(a)). A mixed material layer consisting mainly of the deposited plasma impurity carbon and the substrate material tungsten with a thickness of a few 100 nm is found in both spots of the originally unprotected tungsten surface. After the removal of adsorption layers, an atomic concentration of tungsten of about 30% (Fig. 1(b)) and about 60% (Fig. 1(c)) at a depth of 10 nm is observed. On the other hand, the deposited carbon impurity is found up to a depth of 400 nm. Since the carbon concentration in Fig. 1(b) continuously decreases with depth, it is nearly constant at a tungsten-to-carbon ratio of about two in Fig. 1(c) up to a depth of about 120 nm. Remarkably, the shape of the measured carbon signal (AES) reveals carbide formation at this location.

SIMS imaging demonstrates that the lateral distribution of carbon and tungsten in the mixed layer is

non-uniform. Analyzing regions with a high carbon SIMS signal by AES, we found carbon concentrations up to 66% whereas regions with a low SIMS signal have a carbon concentration of 36% only.

The lateral distribution of carbon and tungsten in the tungsten spot far from the LCFS is more uniform.

3.2. Annealing

AES and SIMS measurements do not indicate any change in the thickness and the atomic composition of the surface layers after annealing the virgin part of the TEXTOR sample at a temperature of 770 K. After

heating the sample to a temperature of 1070 K, the thickness of the carbon layer was found to decrease from 180 to 130 nm. At the interface with the tungsten layer, an intermediate mixed layer consisting of carbon and tungsten was formed (see Fig. 2(a)). The shape of the carbon signal from the AES measurements reveals carbide formation at the interface. Annealing the sample at a temperature of 1370 K resulted in a further reduction in the carbon layer thickness to 60 nm and formation of a W carbide layer with an atomic ratio of W:C close to 2:1 throughout the original tungsten layer (Fig. 2(b)).

3.3. Ion implantation

Fig. 3 shows the depth distribution of carbon and tungsten after irradiation of the solid tungsten specimens with 2.4 keV carbon ions at temperatures 770 and 1070 K, respectively. The bombardment at 770 K caused a carbon film on the tungsten surface with a narrow interface (Fig. 3(a)). In particular, tungsten does not appear at the surface and is only detected below the carbon film. Similar observations were made for all irradiations of the tungsten layer on the polished graphite sample carried out at temperatures up to 970 K.

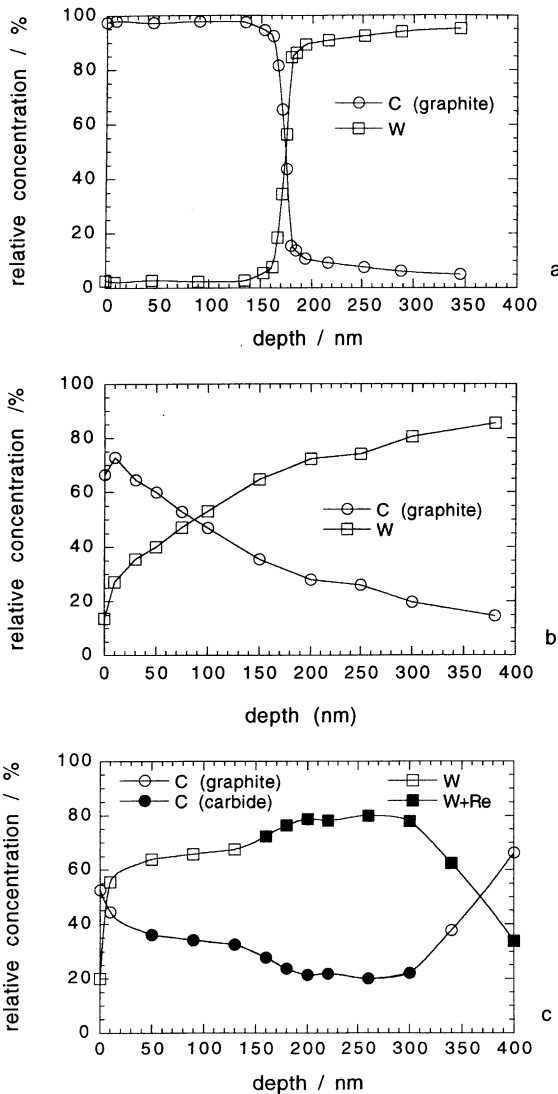


Fig. 1. Depth profiles of carbon and tungsten measured by AES for the a-C:H film: (a) in the covered area and for the contamination layer in the area of both tungsten spots; (b) far from the LCFS; (c) close to the LCFS.

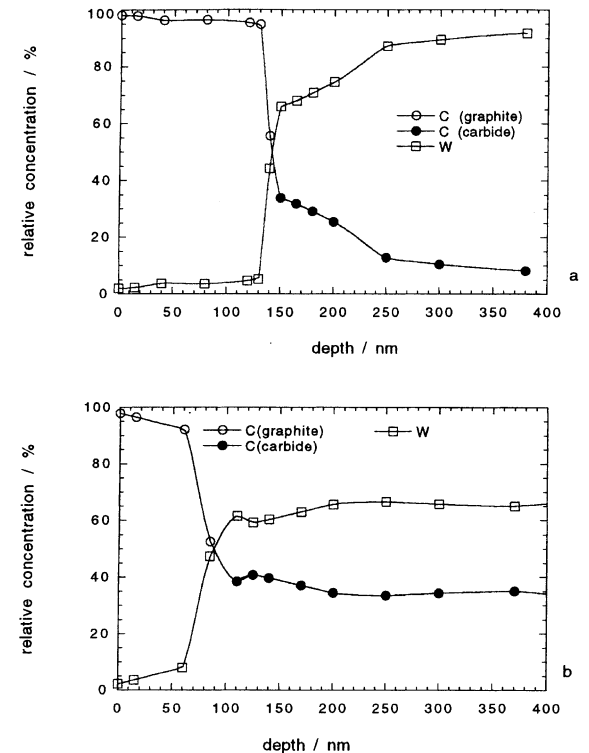


Fig. 2. Depth profiles of carbon and tungsten measured by AES in the covered area of the multi-layer coated TEXTOR-sample: (a) after annealing at 1070 K; (b) after annealing at 1370 K.

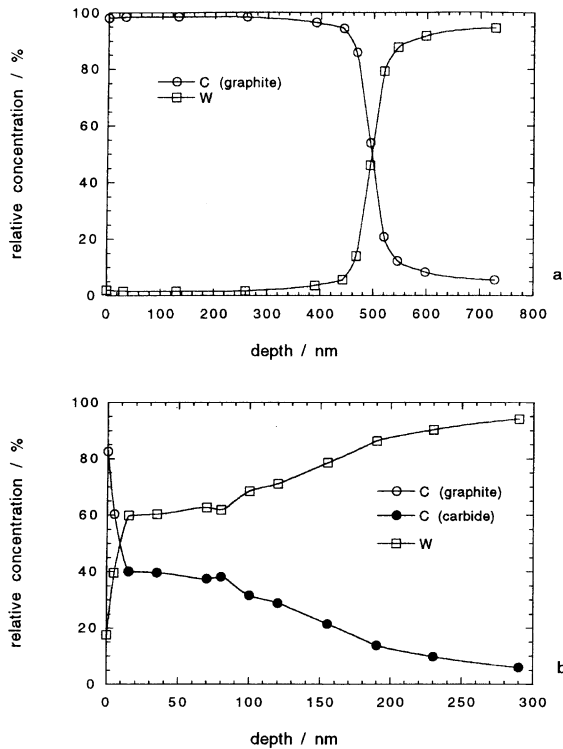


Fig. 3. Depth profiles of carbon and tungsten measured by AES after the implantation of 2.4 keV  $\text{C}^+$  into solid tungsten specimens: (a) after a fluence of  $4.5 \times 10^{22} \text{ C m}^{-2}$  at 770 K; (b) after a fluence of  $2.6 \times 10^{22} \text{ C m}^{-2}$  at 1070 K.

Significant penetration of carbon into the tungsten substrate has been found to be associated with carbide formation for the implantation at 1070 K (Fig. 3(b)).

The simultaneous irradiation of the tungsten surface with carbon and hydrogen ions as realized by the bombardment with  $\text{CH}_3^+$  also caused a carbon coverage of the tungsten surface similar to that shown in Fig. 3(a) when the irradiation was done at room temperature. In particular, the width of the interface region between the carbon layer and the tungsten substrate is as narrow as that at  $\text{C}^+$  bombardment.

At higher temperatures of 770 and 1070 K, the deposited amount of carbon is only a minor fraction of the incident fluence of carbon. Disregarding the adsorbed carbon at the surface, the implanted carbon is found to have penetrated slightly into the tungsten substrate associated with carbide formation. Remarkably, the formation of W carbide was already observed at a temperature of 770 K. However, the implantation at this temperature caused non-uniform carbon deposition. Some small areas of the surface were found to be covered with a mixed material contamination containing implanted carbon without carbide formation up to a depth of 130 nm (see Fig. 4).

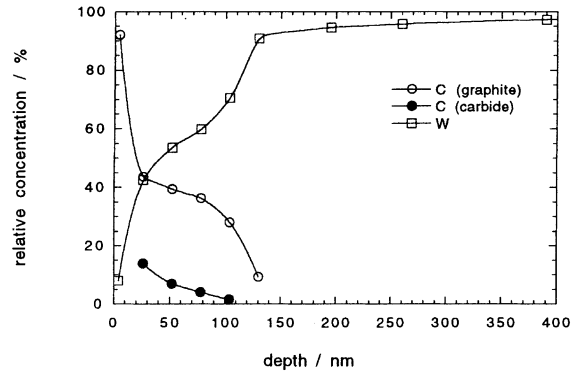


Fig. 4. Depth profiles of carbon and tungsten measured by AES in a selected area after  $\text{CH}_3^+$  implantation with a fluence of  $6 \times 10^{22} \text{ molecules m}^{-2}$  at 770 K.

#### 4. Discussion

In order to explain the material mixing during the plasma exposure in the tokamak experiment, the following processes involved in the growth of the contamination layer are considered: thermal diffusion, penetration during ion bombardment and preferential erosion and redeposition.

The effect of thermal C diffusion into tungsten was investigated by annealing the virgin part of the multi-layer coated graphite sample. The results indicate that a significant penetration of carbon into tungsten occurs at a temperature of 1070 K associated with carbide formation. The atomic ratio of  $\text{W}:\text{C}=2:1$  assigns to ditungsten carbide,  $\text{W}_2\text{C}$ . Other annealing investigations with X-ray photoelectron spectroscopy (XPS) on 3 nm carbon films on tungsten have shown that carbide formation sets in already at a temperature of 770 K, initially with the formation of  $\text{W}_2\text{C}$  [7]. Obviously, carbon penetration starts at higher temperatures and is observable for a temperature of 1070 K in the present experiment.

A quite similar temperature-dependent migration effect was found at implantation of carbon ions.

The incident ion energy of 2.4 keV was chosen to be somewhat higher than the impact energy of  $\text{C}^{4+}$  ions of about 900 eV during plasma exposure ( $2T_i + 3qT_e$  with charge state  $q = 4$ ). For this energy, the implantation ion range is expected to be about 40 nm at normal incidence [8].

This explains the formation of a carbon film with the narrow interface to the tungsten substrate as measured for substrate temperatures up to 970 K during implantation (see Fig. 3(a)). Significant penetration of carbon into tungsten beyond the implantation zone is observed only at a substrate temperature of 1070 K and is found to be associated with ditungsten carbide formation (Fig. 3(b)) as already found in the annealing experiment.

The simultaneous impact of carbon and hydrogen ions also caused a complete carbon film on the tungsten substrate at room temperature. At temperatures 770 and 1070 K, only a minor fraction of the implanted carbon amount is deposited due to the enhanced carbon removal by chemical reerosion [9,10]. The observed carbide formation in a thin surface layer at a temperature of 770 K is in accordance with the results from the XPS-investigations (see above). However, the graphitic carbon found up to a depth of 130 nm demonstrates that carbon can penetrate into the tungsten substrate without carbide formation with simultaneous impact of carbon and hydrogen ions. The carbon contamination after implantation at 1070 K is somewhat higher than that after implantation at 770 K. This may be explained by lower chemical erosion and higher penetration of carbon at 1070 K.

Taking into consideration the results of the annealing and ion irradiation experiments, we can make the following conclusions concerning the growth of the mixed material layer in the tokamak experiment. The mixed layer formed during the tokamak experiment on the tungsten spot near the LCFS obviously results from a temperature excursion during the first two discharges. The tungsten carbide layer found in the area of this spot up to a depth of 120 nm indicates that at least a local surface temperature of about 1070 K was reached. The somewhat lower carbon concentration in the material located deeper than 120 nm can be explained by the fact that this material also contains rhenium as indicated by the SIMS analysis.

No carbide formation and a gradually decreasing carbon concentration with depth have been observed in the area of the tungsten spot far from the LCFS indicating that the local surface temperature was kept below 1070 K. The growth of the mixed material layer in this deposition area seems to be affected by radiation enhanced penetration of carbon at the simultaneous impact of carbon and hydrogen ions as observed in localized regions of irradiation of tungsten with  $\text{CH}_3^+$  ions at 770 K.

Likely, processes such as non-uniform deposition, preferential erosion and redeposition may also contribute to the material mixing at least in the beginning of the coating process. Non-uniform erosion and deposition phenomena during plasma exposure has already been observed on graphite [11,12]. The results from SIMS imaging give evidence of non-uniform carbon deposition on the tungsten surface after the plasma experiment in TEXTOR-94 and indicates that tungsten can be continuously eroded in this case. A considerable fraction of eroded tungsten is redeposited and can be embedded in the carbon contamination. The probability of prompt local redeposition of sputtered and ionized tungsten

atoms is estimated to be about 30% with the plasma parameters during the NBI phase [13]. The total loss of tungsten is estimated to be about  $4 \times 10^{21}$  and  $1 \times 10^{22}$  W atoms  $\text{m}^{-2}$  for the tungsten spots far and near from the LCFS, respectively [3]. Further enrichment of tungsten in the contamination occurs due to the preferential erosion of carbon from the mixed material [12].

## 5. Summary and acknowledgements

The exposure of tungsten surfaces to the carbon-contaminated scrape-off plasma of tokamaks causes the growth of mixed material contamination layers with a thickness much larger than the expected implantation zone. The atomic surface concentration of tungsten is found to be up to 30% even after deposition of  $8 \times 10^{21}$  C atoms  $\text{m}^{-2}$ . At substrate temperatures higher than 1070 K, material mixing is dominated by the diffusion of carbon into tungsten substrates associated with carbide formation as shown by the annealing and implantation experiments during plasma exposure. For lower substrate temperatures, the growth of such layers seems to be affected by ion radiation enhanced penetration of carbon occurring during the simultaneous impact of carbon and hydrogen ions as observed at irradiation of tungsten with  $\text{CH}_3^+$  ions at 770 K. There is indication that processes such as non-uniform carbon deposition prompt local redeposition of eroded tungsten and preferential reerosion of carbon also contribute to material mixing during plasma exposure.

The authors thank J. Roth (MPI für Plasmaphysik, Garching) for fruitful discussions.

## References

- [1] H. Maier et al., J. Nucl. Mater. 266–269 (1999) 1008.
- [2] D. Hildebrandt et al., J. Nucl. Mater. 266–269 (1999) 533.
- [3] D. Hildebrandt et al., in: Proceedings of the 27th EPS Conference on Controlled Fusion and Plasma Physics, Budapest, 2000, to be published.
- [4] P. Wienhold et al., these Proceedings.
- [5] M. Brix, Report of IPP Jülich, Jül-3638, 1998.
- [6] The implanted samples were provided by J. Roth (IPP-Garching).
- [7] J. Luthin, Ch. Linsmeier, Surf. Sci. 454–456 (2000) 78.
- [8] W. Eckstein et al., Nucl. Instrum. and Meth. B 153 (1999) 415.
- [9] K. Krieger et al., these Proceedings.
- [10] W. Wang et al., Nucl. Instrum. and Meth. B 129 (1997) 210.
- [11] P. Wienhold et al., J. Nucl. Mater. 266–269 (1999) 986.
- [12] D. Hildebrandt et al., Phys. Scr. T 81 (1999) 25.
- [13] D. Naujoks, Nucl. Fus. 37 (1997) 1193.